JAAS
Journal of Analytical Atomic Spectrometry

A secondary discharge intensifies optical emission from a Mach disk extracted from an inductively coupled plasma†

Ma'an H. Amad and R. S. Houk*

Ames Laboratory—U. S. Department of Energy, Department of Chemistry, Iowa State University, Ames, IA 50011, USA.
E-mail: rshouk@iastate.edu

The axial channel of a conventional argon inductively coupled plasma (ICP) is extracted through a circular orifice into an evacuated quartz chamber. Emission from the Mach disk region is focused on the entrance slit of an echelle spectrometer equipped with two segmented-array charge-coupled-device detectors. The background pressure in the extraction chamber is 1000 Pa (7.5 torr). At this pressure two barrel shocks and Mach disks are visible. Deliberate use of a mild secondary discharge between the plasma and the sampler enhances emission from the Mach disk for a variety of lines from typical analytes (Ca, Sr, Mg and Mn) by factors of 11 to 25. Detection limits are in the range 0.1–2 μg l^{-1}. Sodium chloride at concentrations up to 10 000 mg l^{-1} induces only a modest loss (0–6%) of intensity for ion lines, in contrast to the much more severe matrix effects seen in ICP mass spectrometry.

Keywords: *Inductively coupled plasma; secondary discharge; Mach disk; supersonic jet; echelle spectrometer; charge-coupled-device detectors; atomic emission spectrometry; inductively coupled plasma mass spectrometry*

Supersonic jet expansions into evacuated chambers have been investigated in many different laboratories.[1–4] Optical emission measurements from a reduced pressure plasma extracted from an analytical ICP were first reported by Lim *et al.*,[5] who showed that ion lines from the supersonic jet were much more prominent than neutral atom lines. The intensities were about 1000 times lower than those observed from the normal analytical zone (NAZ) of an ICP. Ratios of ion to atom line intensity (M II/M I) from the afterglow region were similar to those observed from the NAZ of an ICP.[5] The background emitted by the afterglow was much weaker than that emitted by an ICP. In a second study, the gas kinetic temperature in the Mach disk region was measured to be ≈2200 K.[6]

Previous basic studies of the extraction process for ICP-MS include optical measurements of the extracted gas,[7] photographic studies,[8] gas dynamics,[9] electron density measurements[10] and use of an extraction chamber with an echelle spectrometer and two charge-coupled-device detectors (CCDs).[11] In addition, Borer and Hieftje evaluated the performance of a microwave-boosted reduced-pressure plasma extracted from an atmospheric pressure ICP.[12–14]

In the present paper, the primary objective is to intensify emission from the extracted plasma without increasing the background noise substantially. These measures should improve detection limits compared to those seen previously.[11] The eventual objective of this research is to devise a multielement emission source that produces spectra like those from the ICP itself without the intense continuum background, so that the low dark current of the CCD can be exploited. The present work describes the effect of a mild secondary discharge between the plasma and the sampling orifice[15] on optical emission from the extracted plasma. This discharge is strongest at low power, high aerosol gas flow rate and high water load.[15–19] The discharge also becomes more intense as the sampler is retracted further downstream in the plasma. A mild discharge is expected to accelerate electrons during the extraction process, increase electron temperature[10] and enhance excitation by electron–neutral or electron–ion collisions in the Mach disk. Such collisions should thus enhance the intensities of various emission lines.

† This manuscript contains material presented at the Pittsburgh Conference on Analytical Chemistry and Applied Spectroscopy, Chicago, IL, USA, March 1996.

EXPERIMENTAL

A schematic diagram of the extraction chamber used in this work is shown in Fig. 1. Table 1 summarizes the instrumentation and operating conditions.

ICP instrumentation

The plasma was generated using an external rf generator and matching network, rather than the one supplied with the instrument, for reasons described below. The matching network was mounted on an xyz translation assembly. The torch was turned to the horizontal orientation. The load coil was grounded at the downstream turn to the shielding box, while the other end was connected to the rf output of the matching network.[15] Analyte was introduced into the ICP by a concentric nebulizer (Model TR 30C3, Meinhard Associates, Santa Ana, CA, USA) with a Scott-type spray chamber[20] followed by a desolvation system.[21]

Extraction chamber

The extraction system (Fig. 1) is described in detail in previous publications[5,6,11] and consists of a horizontal ICP that is sampled through a 1.06 mm diameter circular orifice drilled in

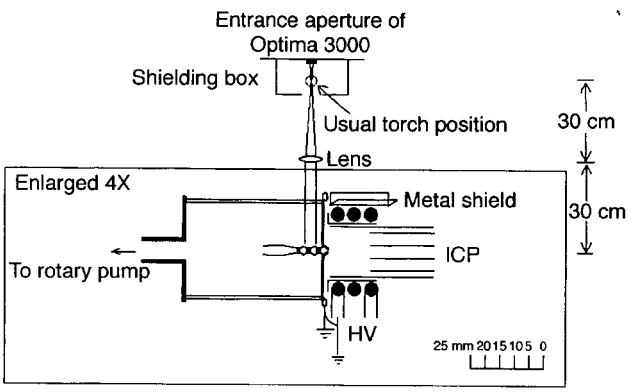

Fig. 1 Schematic diagram of experimental setup. Note that the extraction chamber is to larger scale than the lens and the optical path.

Table 1 Experimental components

Component	Manufacturer/ description	Optimum operating conditions
ICP generator	Type HFP3000D with impedance-matching network Plasma Therm, Inc. Frequency 27.12 MHz	rf power 1.2 kW
ICP torch	Ames Laboratory construction[20]	Aerosol gas flow rate 1.1 l min^{-1} Outer gas 15 l min^{-1} Sample uptake rate 1.0 ml min^{-1}
Nebulizer assembly, spray chamber, desolvation apparatus[21]	Meinhard nebulizer Scott-type, uncooled spray chamber	Heating temperature 100 °C Condenser temperature 0 °C
Sampler	1.06 mm diameter circular orifice in copper disk centered on ICP	Sampling position: 16 mm from load coil on center
Pressure measurement	Convectron vacuum gauge Granville-Phillips 275	Extraction chamber pressure 1000 Pa (7.5 torr)
Vacuum pump	Edwards E2M18 Pumping speed 1.2 l s^{-1}	

a water-cooled copper disk. On the outside of the plate is a quartz cylinder used as the wall of the extraction chamber. The quartz chamber is sealed to the sampling plate with a Viton gasket. The other end of the quartz chamber is sealed to a pumping flange, which is connected to a rotary pump. The copper flange with the orifice was grounded with copper tubing, which also provided cooling water. An inline valve was used to control the pressure in the extraction chamber. The extraction chamber was centered on the ICP. It should be noted that copper emission lines from the sampler were not observed, and the diameter of the sampling orifice did not expand noticeably over a one month period, which indicates the secondary discharge is not strong enough to sputter copper from the sampling orifice.

Optics and detection

A Perkin-Elmer Optima 3000 echelle spectrometer (Norwalk, CT, USA) with a segmented-array CCD[22,23] was used for this experiment. This device provides high quantum efficiency in the UV, low dark current, low read out noise and simultaneous multielement capability.

The generator and coupling box were the same ones used in our initial experiments concerning emission from the Mach disk.[5,6] An external rf generator was necessary because the one supplied with the Optima did not produce a noticeable secondary discharge, as noted previously.[11] The plasma supplied with the Optima was intended for use with a 'free' ICP, *i.e.*, one without a sampling orifice present, and was not designed to either produce or suppress a secondary discharge.

As can be seen in Fig. 1, the extracted plasma is well outside the shielding box of the Optima. To transmit light into the Optima, a quartz lens (f/7) produced a focused image (magnification 1) of the extracted plasma onto the usual position of the torch inside the shielding box of the Optima. This image was then transferred by the entrance optics provided with the Optima. The plasma was blocked by a black metal shield, and the experiments were performed in a dark room to minimize stray light. The section of the extracted plasma viewed is shown in Fig. 2(*b*). The vacuum chamber was grounded carefully to alleviate rf interference.

Reagents

Analyte solutions were prepared by serial dilution of concentrated stock solutions. For Ca, Sr, Mn and Mg, ICP single element stock solutions (Plasma-Chem, Farmingdale, NJ, USA) with analyte concentrations of 50 mg l^{-1} in 2% (v/v) aqueous HNO_3 (J. T. Baker, Phillipsburg, NJ, USA) were used. Solid sodium chloride (analytical grade, Aldrich, Milwaukee, WI, USA) was dissolved into the HNO_3 solutions for the matrix effect studies.

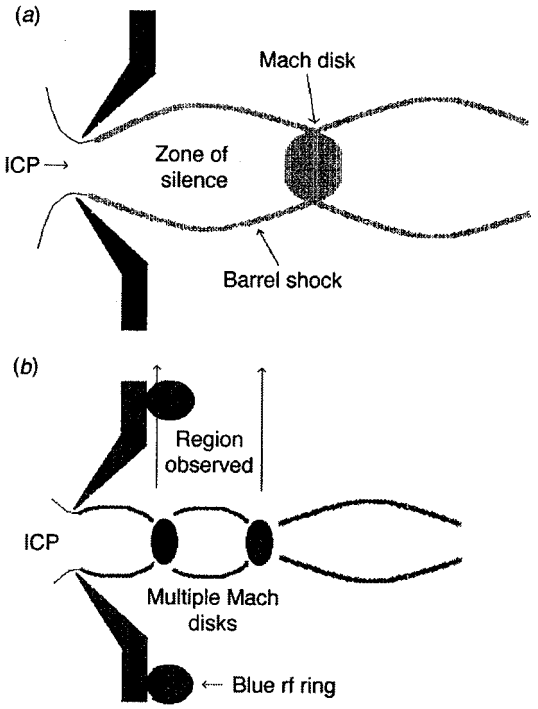

Fig. 2 Close up diagram of supersonic jet and Mach disk: (*a*) pressure = 133 Pa (1 torr), (*b*) pressure = 1000 Pa (7.5 torr). The latter operating pressure was used in the present work.

RESULTS AND DISCUSSION

Structure of the extracted jet

The extracted plasma and shock waves behind the sampling orifice are shown schematically in Fig. 2. With the inline valve open, the pressure is 133 Pa [1 torr, Fig. 2(a)]. The jet consists of the zone of silence surrounded by a faint, diffuse barrel shock and Mach disk. There is no visible emission from inside the zone of silence. The barrel shock and Mach disk are caused

by collisions between fast atoms from the supersonic jet and the background gas. The collisions reheat and scatter the atoms and induce emission.

At a pressure of 1000 Pa [7.5 torr, Fig. 2(b)], the visible structure of the expansion becomes more compact and intense, as described previously by Gray.[8] A second barrel shock and Mach disk form; each is only about 3 mm diameter. Outside the orifice, a dark space about 6 mm in diameter surrounded by a pale blue ring is observed.[7] This ring is probably generated by an rf potential from the ICP induced between the two metal plates of the extraction chamber.

Effect of sampling position on emission from Mach disk

In this study the Mach disk was first located by spatially profiling emission from the extracted plasma. At 7 mm from the sampling orifice, maximum emission was observed from the Mach disk region for various emission lines. Theoretically, the location of the onset of the Mach disk is given by the following equation:[24]

$$X_m/D = 0.67[P_0/P_1]^{1/2} \quad (1)$$

where X_m is the distance of the Mach disk from the sampling orifice, D is the diameter of the sampling orifice (1.06 mm), P_0 is the ICP pressure (10^5 Pa, 760 torr) and P_1 is the background pressure in the extraction chamber. The orifice used here was 1.06 mm in diameter and the pressure in the extraction chamber was 1000 Pa (7.5 torr), which should produce the first Mach disk at $X_m = 7.05$ mm, in good agreement with the observed maximum in emission intensity at 7 mm.

The variation of net intensity of various atom (I) and ion (II) lines with sampler–load coil separation (*i.e.*, sampling position) at constant chamber pressure (1000 Pa, 7.5 torr), aerosol gas flow rate (1.1 l min^{-1}) and power (1.1 kW) is shown in Fig. 3. This experiment is performed by moving the plasma relative to the sampler and observation region, which are fixed relative to the spectrometer. Moving the plasma changes both the plasma region sampled by the vacuum chamber and the severity of the secondary discharge.

As shown in Fig. 3, the line intensities maximize when the sampler is 15–17 mm from the load coil. The spatial emission profile for Ca I 422.673 is double humped, with the main peak at 16–17 mm and a weak one at 25 mm. The profiles of the other lines studied (Ca II, Mg I, Mg II, Sr I, Sr II, Mn I, Mn II) have a single hump shape with maximum intensity at 15–17 mm. A mild secondary discharge can be seen between the plasma and the sampling cone at a sampling position of 15 mm or further from the load coil. The discharge in the present work is visually much weaker than that described previously for enhancing emission intensity outside the sampler in the ICP.[15–19]

Effect of power

The variation of line intensity with power at constant sampling position (15 mm), aerosol gas flow rate (1.0 l min^{-1}) and pressure (7.5 torr) is shown in Fig. 4. The Ca I line (422.676 nm) maximizes at low power (0.9 kW). Strontium atom I and ion II lines reach maxima at 1.2 kW. The Mg I line intensity maximizes at 1.2 kW and then plateaus off as power increases further. This plateau might be due to the fact that as power increases the strength of the discharge decreases.[15] Meanwhile, the intensities of the Mn atom and ion lines increase similarly as forward power increases. A power of 1.2 kW is suitable for multielement work with only a minimal compromise in signal, especially for ion lines, as is the case when emission is observed from the ICP itself.

Effect of aerosol gas flow rate

The effect of aerosol gas flow rate on analyte net intensity from the Mach disk at constant sampler–load coil separation

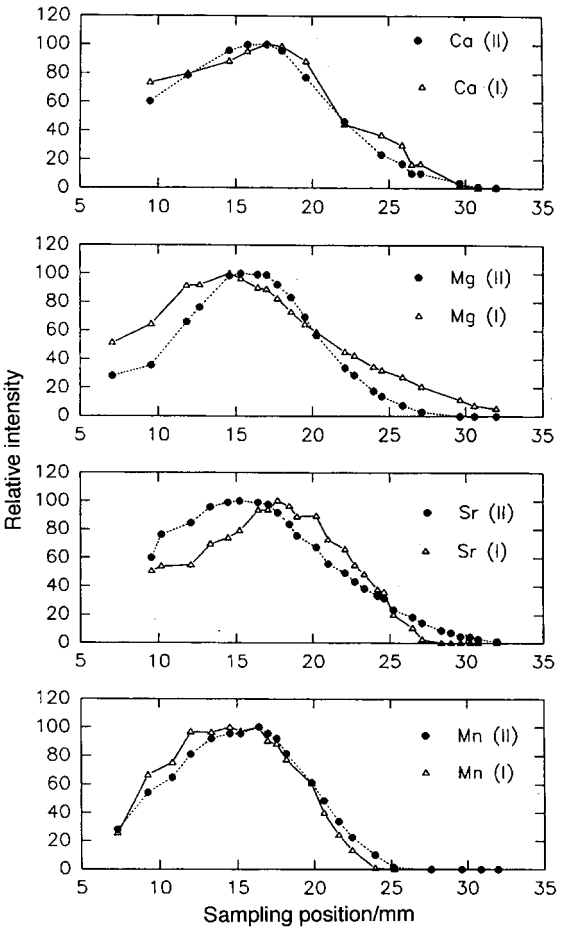

Fig. 3 Effect of sampling position on emission intensity from Mach disk. Specific wavelengths are given in Table 2. The analyte concentrations were 50 mg l^{-1}, and the intensities are normalized in these and subsequent figures.

(15 mm), forward power (1.2 kW) and pressure (7.5 torr) is shown in Fig. 5. The profile of analyte ion line intensity as a function of aerosol gas flow rate is a single hump with a maximum located between 1.0–1.1 l min^{-1}. The profiles for analyte atom lines are different from those for ion lines. The plots for Ca I and Sr I lines have two humps at 1.0–1.2 l min^{-1} and 1.6 l min^{-1}. The second hump appears at 1.4 l min^{-1} for the Mg I line. Surprisingly, the profiles for both Mn I and Mn II lines are single sharp peaks with maxima at 1.2 l min^{-1}.

Presumably, the number density of metal ions (M^+) and excitation temperature (T_{exc}) are related to the corresponding quantities outside the sampler in the ICP.[11] Thus, the intensity of metal ion lines from the Mach disk can be generalized by the following proportionality:[11]

$$(I_{M+})_{MD} \propto (n_{M+})_{MD} \exp(-E^*/kT_{exc}) \quad (2)$$

where MD refers to the Mach disk, E^* is the excitation energy (measured relative to the lowest level of the ion) and k is the Boltzmann constant.

The data presented in Fig. 5 can be rationalized from combining this proportionality with the concept that the section of the axial channel that passes through the orifice and the severity of the secondary discharge both change with aerosol gas flow rate. When the aerosol gas flow rate is 1.1 l min^{-1} and sampling position is 15 mm, the discharge is visible outside the sampler. The potentials that accompany this mild discharge accelerate electrons during the extraction process, which increases electron temperature, T_{exc} and the fraction of excited M^+ ions in the Mach disk. Furthermore, at this sampling position the tip of the initial radiation zone

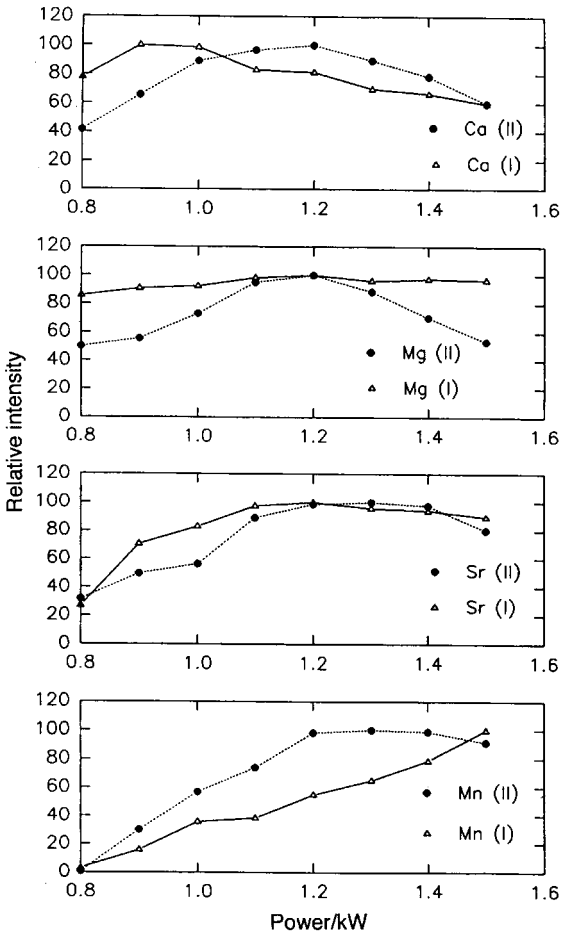

Fig. 4 Dependence of analyte line intensity on power.

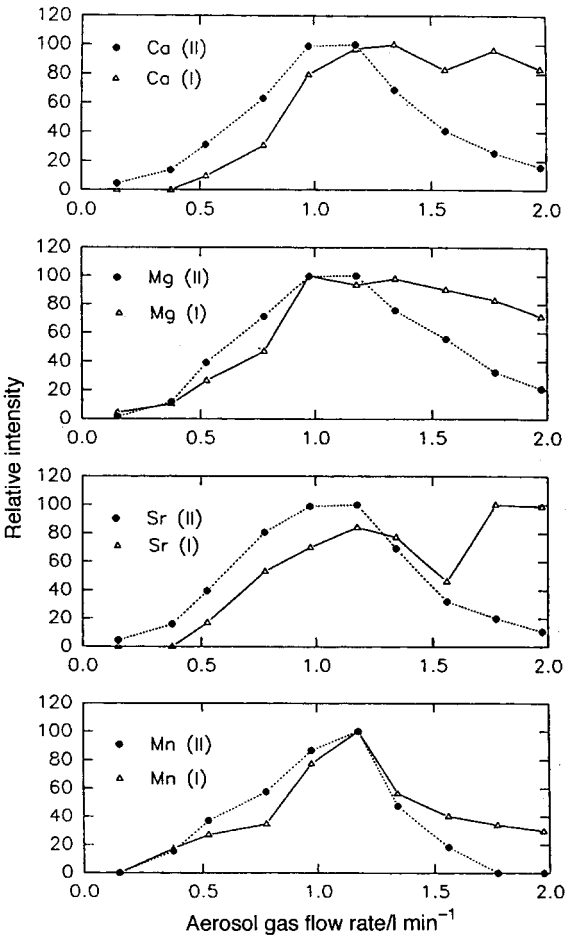

Fig. 5 Dependence of analyte line intensity on aerosol gas flow rate.

(IRZ)[25] is about 1–2 mm upstream from the sampling orifice. This is roughly the same sampling position that maximizes ion signal in ICP-MS.[26,27] Thus, ion lines in particular are enhanced at 1.1 l min^{-1}.

At low aerosol gas flow rate ($\approx$0.5 l min^{-1}), less total analyte reaches the plasma, the sampler is too far downstream from the IRZ and the sampler is at a position where the analyte stream has spread out considerably. The secondary discharge is still present but too weak to be visible, as is the case with most ICP-MS devices that do not employ a balanced or shielded load coil. Thus, both the density factor n_{M+} and the Boltzmann factor in eqn. 2 are reduced, and emission intensity is low. At extremely high aerosol gas flow rate (1.6–1.7 l min^{-1}), the discharge is strong but the sampling orifice is well inside the IRZ, where there are few M^+ ions. These conditions produce highest emission from neutral atoms at the expense of ion emission.

Ion to atom line intensity ratios

The figures discussed to this point are intended primarily for optimization purposes and therefore show only normalized intensities. The effect of the secondary discharge on ion : atom intensity ratios is presented in Table 2. In general, the ion : atom intensity ratios from the Mach disk generated in the present work were higher than those seen with the Mach disk produced using the plasma supplied with the Optima, except for the intensity ratio Ca II 396.847/Ca I 422.673, which is perhaps a bit lower in the present work. This enhancement in ion line intensity is attributed to the fact that a mild discharge accelerates electrons during the extraction process, which increases electron temperature (T_e) and T_{exc} in the observed region of the extracted plasma, as described above.

Table 2 Ion : atom line intensity ratios from the Mach disk compared to those obtained without a secondary discharge[11]

	Intensity Ratio	
Line pair/nm	Present work	Previous work[11]
Ca II 393.366/Ca I 422.673	28	22
Ca II 396.847/Ca I 422.673	3.5	4.5
Mg II 279.533/Mg I 285.213	11	4.5
Mg II 280.270/Mg I 285.213	4.5	1.5
Sr II 407.771/Sr I 460.733	33	22
Sr II 421.552/Sr I 460.733	10	7
Mn II 257.610/Mn I 279.482	6	*
Mn II 260.569/Mn I 279.482	3	*

* Not measured in ref. 11.

Mermet[28] suggests the use of the intensity ratio Mg II 280.270 nm/Mg I 285.213 nm as a simple test of the 'robustness' of atomization and excitation conditions in an ICP. This ratio should $\gtrsim$10 if the plasma is operated under 'robust' conditions. In our experiment, this intensity ratio is 4.5 (Table 2). It should be noted that intensity ratios measured in this study can not be directly compared to those values observed from the NAZ of an ICP[29] due to the variable sensitivity of different subarrays in the CCD. These two Mg lines are detected on different subarrays. Different lines are also measured in different orders in the echelle configuration, which also complicates comparison with ion : atom intensity ratios determined using other instruments. Thus, the Mg II/Mg I intensity ratio observed with our particular Optima from the normal analytical zone of an ICP is approximately 3.7. The value of 4.5 shown in Table 2 from the Mach disk is actually higher than that seen from the ICP

Table 3 Sensitivities (Z_a) and detection limits

Element and line	Z_a/ counts s^{-1} per $\mu g\ l^{-1}$	Z_b/ counts s^{-1}	σ/ counts s^{-1}	Detection limits/$\mu g\ l^{-1}$		
				Present work	Previous work[11]	ICP+ Optima†
Ca II 393.366	1.1×10^5	4.12	0.0694	0.10	2	0.4
Mg II 279.553	2.3×10^4	4.01	0.0705	0.4	6	0.4
Sr II 407.771	6.3×10^4	4.87	0.0425	0.1	4	0.1
Mn II 257.610	3250	5.11	0.0523	2	*	2

Z_a is the peak intensity of the analyte line after background correction. The analyte concentration is 50 ppm. Z_b is the spectral background at the peak maximum. σ is the standard deviation of the blank for 11 replicates. The detection limit is the solution concentration necessary to produce a net signal equal to three times the standard deviation of the blank. † These values are detection limits listed for the Optima during lateral viewing of emission from the conventional ICP.[30] * Not measured in ref. 11.

itself with our particular spectrometer, in agreement with our earlier observations.[5,10] We therefore conclude that the Mach disk is at least as 'robust' as the ICP in the Optima, according to Mermet's criterion.

Detection limits

The limit of detection (LOD) is defined as the concentration necessary to produce a net signal equivalent to three times the standard deviation of the background. The LODs obtained in this study are shown in Table 3. Standard deviation (σ) was calculated for 11 consecutive measurements with an integration time of 200 s for each line. The values are measured for the most intense line for each element under the multielement operating conditions listed in Table 1. LODs in the range 0.1–2 g μl^{-1} were obtained.

The LODs obtained in the present work are better than the range of 2–6 $\mu g\ l^{-1}$ previously obtained by Shen *et al.*[11] The reasons are illustrated by the data in Table 4, which shows the effect of the secondary discharge on sensitivity, background, noise and LODs. In general, the mild discharge enhanced analyte line intensity by factors of 11 to 25, even though use of the external rf generator forced us to put the Mach disk a substantial distance from the entrance slit (see Fig. 1). Thus, the light throughput is probably poorer in the present work than in that reported previously,[11] when the vacuum chamber was inside the usual shielding box of the Optima.

Meanwhile, the secondary discharge increased the background by factors of 10 to 26. The increase in background is presumably due to the stronger white continuum emission from the Mach disks and also to the blue ring around the plate containing the sampling orifice (see Fig. 2). The blue ring is prominent only when there is a substantial secondary discharge.

Although the background emitted by the Mach disk is elevated twentyfold by the secondary discharge, the noise on the background is not changed appreciably. Thus, LODs for the elements studied are better than those obtained by Shen *et al.*[11] while viewing the Mach disk without the secondary discharge. Our new LODs are also about the same as those obtained by the Optima 3000 during lateral viewing of the ICP alone.[30]

Table 4. Effect of secondary discharge on sensitivity, background, noise and detection limits

Element and line	Z_a ratio	Z_b ratio	σ ratio	LOD ratio
Ca II 393.366	23	25	0.96	0.05
Mg II 279.553	11	20	0.87	0.016
Sr II 407.771	24	26	0.67	0.06

Z_a ratio is (net intensity with secondary discharge)/(net intensity from ref. 11, no secondary discharge). The other ratios are defined similarly. Z_b is the net peak intensity of the spectral background at the peak maximum. σ is the standard deviation of the blank for 11 replicates. LOD is the solution concentration necessary to produce a net signal equal to three times the standard deviation of the blank.

Effect of sodium matrix on analyte line intensity

The effect of sodium concomitant on analyte signals is shown in Fig. 6. The optimized operating conditions described above were used for these experiments and are identified in the figure caption. Blanks of the most concentrated matrix solutions were analyzed and did not have significant amounts of the analytes.

The two plots at the top of Fig. 6 show that the intensity of the Ca II line at 393.366 nm is not affected substantially by the Na matrix at concentrations up to at least 10 000 mg l^{-1}

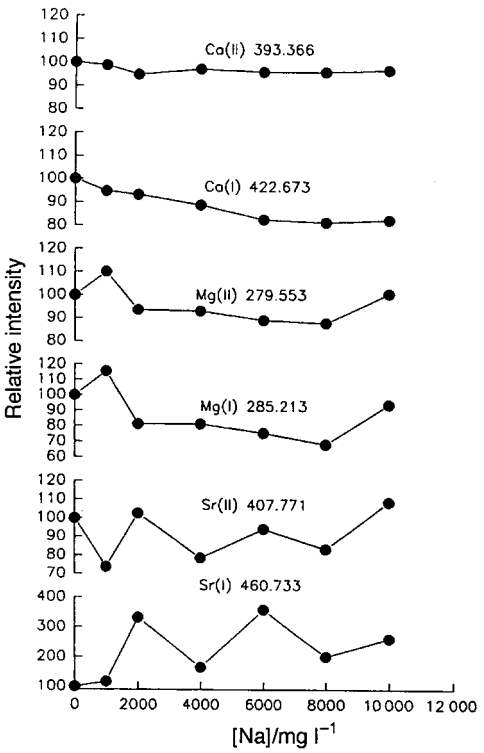

Fig. 6 Effect of sodium concomitant on analyte line intensity under multielement operating conditions. The analyte concentrations were 50 mg l^{-1}.

Na, *i.e.*, a 1% Na solution. The intensity of the Ca I line at 422.673 nm is suppressed by about 15% at 10 000 mg l^{-1} Na. For both Mg II and Mg I lines, an odd enhancement is seen at 1000 mg Na l^{-1}, followed by a modest suppression of signal. The behavior of strontium signal with sodium concentration is erratic. For Sr II 407.771 nm, the various points average to a modest suppression of about 10%, whereas the Sr I line is enhanced in the presence of the Na matrix. It is odd that the sodium matrix should enhance the intensity of the Sr I line and suppress that of the Ca I line.

For the ion lines and the relatively high energy neutral atom line Mg I 285.213, the matrix effects shown in Fig. 6 are similar in magnitude to those that would be expected if emission were observed from the ICP alone under multielement operating conditions.[15] These are the most sensitive lines for these elements and would be the preferred ones for analytical use.

The matrix effects shown in Fig. 6 are comparable to those seen in the early work of Lim and Houk[5] and are much less severe than those that would be seen by ICP-MS.[31] We suggest that the moderate severity of the matrix effect in the present work is the result of juxtaposition of two competing phenomena. Sodium at these concentrations would be expected to cause a substantial loss of analyte ions in the plasma itself, according to the measurements of Hobbs and Olesik.[32] It is difficult to estimate the extent of loss of analyte ions directly from their data, since (a) they report results for Li and Ba but not for a Na matrix itself, and (b) the plasma they used did not have a sampling orifice present. Nevertheless, sodium at 10 000 mg l^{-1} Na should suppress the analyte ion density in the ICP by at least a factor of two. Taken alone, this effect should then suppress the signal for analyte ions from the Mach disk.

Some opposing phenomenon must then excite the ions more efficiently to offset this expected loss of analyte ions. Hieftje and co-workers report Thomson scattering measurements that show that T_e along the central axis of the ICP actually increases when an alkali metal matrix is added.[33] Previous Langmuir probe measurements show that changing plasma conditions that increase the plasma potential and intensity of the secondary discharge cause a corresponding increase in T_e in the supersonic jet.[10,34] Thus, addition of sodium could increase electron temperature in both the plasma and the Mach disk. The presence of more energetic electrons in the Mach disk should boost the populations of excited levels of analyte ions and thus compensate for the expected suppression in analyte ion density. Since this second process primarily produces a higher fraction of ions in excited states, rather than more total ions, it does not influence matrix effects in ICP-MS, which are substantially more severe than those seen in the present work.

CONCLUSION

The present work shows that inducing a mild secondary discharge improves LODs by increasing line intensities without also increasing the noise on the background. Additional improvements in LODs could therefore be possible if the intensities could be boosted further. The Mach disk source also benefits from similar tolerance to matrix effects induced by sodium as the ICP itself. However, the LODs in the present work are improved only to the point where they are comparable to those obtained from conventional lateral viewing of the ICP, *i.e.*, they are not yet competitive with the performance of axially-viewed ICP emission spectrometry or ICP-MS. It must also be admitted that the lines measured are relatively easily excited. Thus, although the Mach disk emission source shows some promise, further development is necessary before it represents any improvement over the existing ICP.

Ames Laboratory is operated by Iowa State University for the U. S. Department of Energy under Contract No.W-7405-ENG-82. This work was supported by the Office of Basic Energy Sciences, Division of Chemical Sciences. The authors thank Perkin-Elmer for the loan of the Optima.

REFERENCES

1 Anderson, J. B., in *Molecular Beams and Low Density Gas Dynamics*, ed Wegener, P. P., Marcel Dekker, New York, 1974, p. 1.
2 Kantrowitz, A., and Grey, J., *Rev. Sci. Instrum.*, 1951, **22**, 328.
3 Knuth, E. L., *Appl. Mech. Rev.*, 1964, **17**, 751.
4 Houk, R. S., Fassel, V. A., Flesch, G. D., Svec, H. J., Gray, A. L., and Taylor, C. E., *Anal. Chem.*, 1980, **52**, 2283.
5 Houk, R. S., and Lim, H. B., *Anal. Chem.*, 1986, **58**, 3244.
6 Lim, H. B., Houk, R. S., Edelson, M. C., and Carney, K. P., *J. Anal. At. Spectrom.*, 1989, **4**, 365.
7 Kawaguchi, H., Asada, K., and Mizuike, A., *Mikrochim. Acta*, 1988, **III**, 143.
8 Gray, A. L., *J. Anal. At. Spectrom.*, 1989, **4**, 371.
9 Douglas, D. J., and French, J. B., *J. Anal. At. Spectrom.*, 1989, **4**, 371.
10 Lim, H. B., and Houk, R. S., *Spectrochim. Acta, Part B*, 1990, **45**, 453.
11 Luan, S., Pang, H.-M., and Houk, R. S., *J. Anal. At. Spectrom.*, 1996, **11**, 247.
12 Borer, M. W., and Hieftje, G. M., *Spectrochim. Acta, Part B*, 1991, **14**, 463.
13 Borer, M. W., and Hieftje, G. M., *J. Anal. At. Spectrom.*, 1993, **8**, 333.
14 Borer, M. W., and Hieftje, G. M., *J. Anal. At. Spectrom.*, 1993, **8**, 339.
15 Gray, A. L., Houk, R. S., and Williams, J. G., *J. Anal. At. Spectrom.*, 1987, **2**, 13.
16 Olivares, J. A., and Houk, R. S., *Appl. Spectrosc.*, 1985, **39**, 1070.
17 Lim, H. B., Carney, K. P., Edelson, M. C., Houk, R. S., and Brenner, I. B., *Spectrochim. Acta, Part B*, 1993, **48**, 1617.
18 Houk, R. S., LaFreniere, B. R., Lim, H. B., and Fassel, V. A., *Appl. Spectrosc.*, 1987, **41**, 391.
19 Tan, H., Ishii, I., and Montaser, A., *J. Anal. At. Spectrom.*, 1991, **6**, 317.
20 Scott, R. H., Fassel, V. A., Kniseley, R. N., and Nixon, D. E., *Anal. Chem.*, 1974, **46**, 75.
21 Fassel, V. A., and Bear, B. R., *Spectrochim. Acta, Part B*, 1986, **41**, 1089.
22 Barnard, T. W., Crockett, M. I., Ivaldi, J. C., and Lundberg, P. L., *Anal. Chem.*, 1993, **65**, 1225.
23 Barnard, T. W., Crockett, M. I., Ivaldi, J. C., Lundberg, P. L., Yates, D. A., Levine, P. A., and Dauer, D. J., *Anal. Chem.*, 1993, **65**, 1231.
24 Ashkenas, H., and Sherman, F. S., in *Rarefied Gas Dynamics Proc. 4th Int. Symp. Rarefied Gas Dynamics*, ed. De Leeuw, J. H., Academic Press, New York, 1966, vol. II, pp. 84–105.
25 Koirtyohann, S. R., Jones, J. S., and Yates, D. A., *Anal. Chem.*, 1980, **52**, 1966.
26 Vaughan, M.-A., Horlick, G., and Tan, S. H., *J. Anal. At. Spectrom.*, 1987, **2**, 765.
27 Horlick, G., Tan, S. H., Vaughan, M. A., and Rose, C. A., *Spectrochim. Acta, Part B*, 1985, **40**, 1555.
28 Mermet, J. M., *Anal. Chim. Acta*, 1991, **250**, 85.
29 Winge, R. K., Fassel, V. A., Peterson, V. J., and Floyd, M. A., *Inductively Coupled Plasma-Atomic Emission Spectroscopy. An Atlas of Spectral Information*, Elsevier, Amsterdam, 1985, Appendix A.
30 Optima 3000 Wavelength Tables, Perkin-Elmer Corporation, 1993.
31 Olivares, J. A., and Houk, R. S., *Anal. Chem.*, 1986, **58**, 20.
32 Hobbs, S. E., and Olesik, J. W., *Spectrochim. Acta, Part B*, 1993, **48**, 817.
33 Hanselman, D. S., Sesi, N. N., Huang, M., and Hieftje, G. M., *Spectrochim. Acta, Part B*, 1994, **49**, 495.
34 Lim, H. B., Houk, R. S., and Crain, J. S., *Spectrochim. Acta, Part B*, 1989, **44**, 989.

Paper 7/04272H
Received June 18, 1997
Accepted February 3, 1998